

5-2023

## Spatial Variability of Alkali-metal Polarization

Lauren Vannell  
*William & Mary*

Follow this and additional works at: <https://scholarworks.wm.edu/honorstheses>



Part of the [Atomic, Molecular and Optical Physics Commons](#)

---

### Recommended Citation

Vannell, Lauren, "Spatial Variability of Alkali-metal Polarization" (2023). *Undergraduate Honors Theses*. William & Mary. Paper 2052.  
<https://scholarworks.wm.edu/honorstheses/2052>

This Honors Thesis -- Open Access is brought to you for free and open access by the Theses, Dissertations, & Master Projects at W&M ScholarWorks. It has been accepted for inclusion in Undergraduate Honors Theses by an authorized administrator of W&M ScholarWorks. For more information, please contact [scholarworks@wm.edu](mailto:scholarworks@wm.edu).


# Spatial Variability of Alkali-metal Polarization

A thesis submitted in partial fulfillment of the requirement  
for the degree of Bachelor of Science with Honors in  
Physics from the College of William and Mary in Virginia,

by

Lauren Vannell

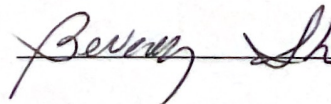
Accepted for Honors



Advisor: Prof. Todd Averett



Prof. Keith Griffioen



Prof. Beverly Sher

Williamsburg, Virginia  
May 3 2023

# Contents

List of Figures	iii
Abstract	v
<b>1 Introduction</b>	<b>1</b>
1.1 Goal of the Experiment . . . . .	1
<b>2 Theory</b>	<b>3</b>
2.1 Faraday Rotation . . . . .	3
2.2 Voigt Effect . . . . .	4
2.3 Path Length Correction . . . . .	6
<b>3 Experimental Technique</b>	<b>7</b>
3.1 Faraday Rotation . . . . .	7
3.2 Voigt Effect . . . . .	8
<b>4 Results and Conclusions</b>	<b>10</b>
4.1 Results . . . . .	10
4.1.1 Simulated Faraday Rotation . . . . .	10
4.1.2 Faraday Rotation . . . . .	10
4.1.3 Voigt Effect . . . . .	11
4.2 Error Analysis . . . . .	14

4.3 Plans for Future Work . . . . .	15
<b>References</b>	<b>21</b>

# List of Figures

1.1	D2 Fluorescence in a Cell . . . . .	2
2.1	Voigt Effect Diagram . . . . .	5
3.1	Experimental Set-up: FR Photodiode System . . . . .	8
3.2	Experimental Set-up: FR Polarimeter System . . . . .	9
3.3	Experimental Set-up: VR Polarimeter System . . . . .	9
4.1	Photodiode signals from simulated Faraday Rotation using a half-wave plate . . . . .	11
4.2	Calculated asymmetry from simulated Faraday Rotation using a half-wave plate . . . . .	12
4.3	Relationship between PD diff signal and difference . . . . .	13
4.4	Photodiode signals from Faraday Rotation due to change in alkali polarization . . . . .	14
4.5	Calculated asymmetry from Faraday Rotation due to change in alkali polarization . . . . .	15
4.6	VR range for different probe wavelengths . . . . .	16
4.7	VR from varied alkali polarization (793.77nm) . . . . .	17
4.8	VR across cell at varied pump laser power (793.77nm) . . . . .	18
4.9	VR across cell at varied pump laser power (pumped both sides, 793.77nm) . . . . .	19
4.10	D2 Fluorescence in a Cell (both sides) . . . . .	20

## **Abstract**

An experiment was conducted at William & Mary to study how alkali polarization varies spatially in a spherical cell during the process of optical pumping. Similar cells are used to study the neutron via electron scattering from polarized  $^3\text{He}$  nuclei, and those experiments could be improved if alkali polarization is maximized and uniformly distributed throughout the cell. The results of this experiment indicate that the alkali polarization is non-uniform and more heavily concentrated on the side of the cell facing the pump laser.

# Chapter 1

## Introduction

### 1.1 Goal of the Experiment

The goal of this project is to measure and maximize the polarization of alkali vapor in a spherical glass cell during the process of optical pumping. These cells are used for electron scattering experiments at Jefferson Lab. Through a chain reaction, circularly polarized light from a pump laser can be used to polarize the neutron in the nucleus of  $^3\text{He}$  atoms in an external magnetic field. Light first polarizes the alkali atoms, rubidium (Rb), which in turn polarize the  $^3\text{He}$  nuclei through collision. Rb polarization is near-instantaneous, while  $^3\text{He}$  polarization takes time. The pump laser continuously polarizes the Rb, keeping the alkali polarization at a maximum [1]. Polarization of the  $^3\text{He}$  is mainly dependent on its depolarization rate, the Rb to He spin exchange rate, and the average polarization of alkali in the cell. To obtain an ideal cell with  $^3\text{He}$  polarization of approximately 100 percent, average alkali polarization of 100 percent and a very low depolarization rate are required. The average Rb polarization is thought to be 100 percent, and the depolarization rate is determined by the quality of the glass cell. By recording the time it takes the  $^3\text{He}$  to depolarize once the laser and heat are removed (the “lifetime” of the cell), the depolarization rate can be measured. However, even as cells with longer lifetimes are made, the  $^3\text{He}$

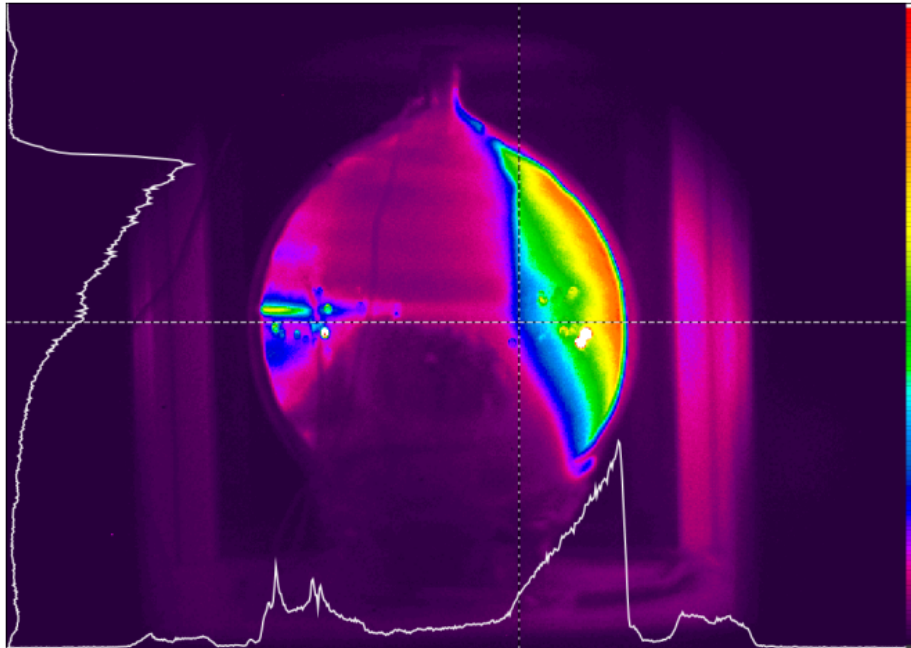


Figure 1.1: **D2 Fluorescence in a Cell.** D2 fluorescence in a spherical cell measured during optical pumping. Light intensity is indicated with a color gradient. The light is concentrated almost entirely on the side of the cell facing the pump laser, implying that alkali polarization is less than 100 percent and non-uniform.

polarization has not exceeded 60 percent, leading to speculation about the average Rb polarization [2].

As Rb is polarized, it fluoresces with D2 light. By using a camera and analysis software, this light can be imaged within the cell, along with its spatial distribution. Tests have shown that the D2 light is very concentrated in one area of the cell, and not evenly distributed, as shown in Figure 1.1. This uneven distribution could mean that polarization is also only occurring in a small portion of the cell rather than the entire volume [4]. The polarization in a specific location of the cell can be determined by measuring the Faraday Rotation or the Voigt Effect with a low-power linearly polarized probe laser.



# Chapter 2

## Theory

### 2.1 Faraday Rotation

The general electric field of polarized light propagating in the  $\hat{z}$  direction in free space is given by the equation

$$\vec{E} = (E_{0x}\hat{x} + E_{0y}\hat{y})e^{i(\tilde{k}z - \omega t)},$$

which can be reduced to a single component when the direction of polarization is set to only one coordinate. For the case of light propagating in the  $\hat{z}$  direction and an external magnetic field also pointing in the  $\hat{z}$  direction, the initial and final electric fields after traveling through alkali vapor are given by the equations

$$\vec{E}_0 = E_{0x}\hat{x}e^{i(\tilde{k}z - \omega t)},$$

$$\vec{E}_f = (E_{fx}\hat{x} + E_{fy}\hat{y})e^{i(\tilde{k}z - \omega t)},$$

with  $\tilde{k} = k + i\kappa$ . The polarization of the light is linear before entering the cell. After exiting the cell, the polarization is still linear, but rotated. Because of circular birefringence, the refractive indices of left and right circularly polarized light are not equal. Birefringence comes from the polarizability of alkali atoms in the presence of the electric field of incident light [5]. The absorption coefficients are also different for the two polarizations. Therefore instead of  $\hat{x}$  and  $\hat{y}$ , a basis of left and right

circular polarization can be used. The end result of polarized light produced by a low-power probe laser passing through a cell is rotation of the incident  $\vec{E}_0$  direction and attenuation. For a detailed description, see Ref [5].

The equations for the Faraday Rotation angle and attenuation are given by

$$\phi_r = C_r \frac{P[A]\ell}{\lambda} f(\lambda, \lambda_{D1}, \lambda_{D2})$$

$$\beta_r = \frac{C_r}{2} \frac{P[A]\ell}{\lambda} g(\lambda, \lambda_{D1}, \lambda_{D2}).$$

Where  $C$  is a constant,  $P$  is the alkali polarization,  $[A]$  is the alkali density,  $\lambda$  is the wavelength, and  $\ell$  is the distance traveled through the alkali vapor. Functions  $f$  and  $g$  make a correction for proximity to resonance. The light that emerges from the cell can be decomposed into two orthogonal components,  $E_x$  and  $E_y$ , the intensities of which are related to the Faraday Rotation and attenuation,

$$\frac{|E_x|^2 - |E_y|^2}{|E_x|^2 + |E_y|^2} = \frac{\cos(2\phi_r)}{\cosh(2\beta_r)}.$$

## 2.2 Voigt Effect

For the case of light propagating in the  $\hat{x}$  direction and a magnetic field pointing in the  $\hat{z}$  direction, one component of the electric field is parallel to the magnetic field, while the other is normal to it. Because of linear dichroism, the absorption of light polarized parallel and light polarized perpendicular to the field are not equal. The  $\hat{y}$  component of the electric field normal to the external magnetic field is not affected; only the  $\hat{z}$  component parallel to the magnetic field is absorbed. The absorption of only one component of a vector causes a rotation in the polarization angle, similar to Faraday Rotation as seen in Figure 2.1. However, the polarization vector also shrinks as it rotates, limiting measurements to those within a 90 degree window. The maximum signal is produced when the initial polarization angle is 45 degrees [6].

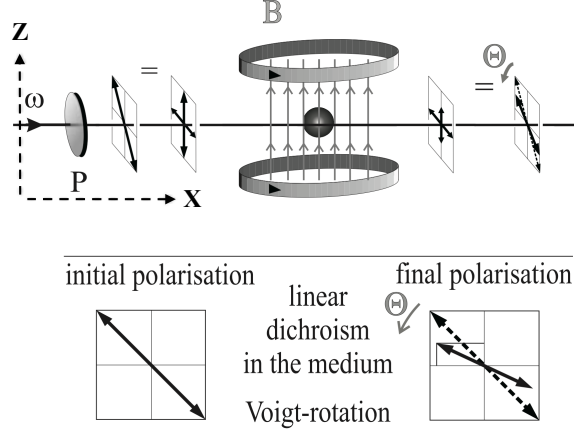


Figure 2.1: **Voigt Effect Diagram.** Experimental configuration for the Voigt Effect is shown [6]. The same set-up is used for Faraday Rotation, but with the probe laser incident from  $\hat{z}$  direction.

The initial and final electric fields after traveling through alkali vapor are given by the equations

$$\vec{E}_0 = (E_{0y}\hat{y} + E_{0z}\hat{z})e^{i(\vec{k}x - \omega t)}$$

$$\vec{E}_f = (E_{0y}\hat{y} + E_{fz}\hat{z})e^{i(\vec{k}x - \omega t)},$$

where the end result of polarized light passing through the cell is again rotation of the incident  $\vec{E}_0$  direction and attenuation. The rotation produced by the Voigt Effect is also proportional to the alkali polarization

$$\phi_v = C_v \frac{P[A]\ell}{\lambda} h(\lambda, \lambda_{D1}, \lambda_{D2})$$

$$\beta_v = \frac{C_v}{2} \frac{P[A]\ell}{\lambda} j(\lambda, \lambda_{D1}, \lambda_{D2}).$$

Where functions  $h$  and  $j$  make a correction for proximity to resonance.

## 2.3 Path Length Correction

After the rotation is measured at different locations in the spherical cell, the path length changes and a correction must be made to the Voigt Effect equation. The new path length can be found using the formula for chord length:

$$\ell = 2\sqrt{r^2 - d^2},$$

where  $r$  is the radius of the sphere,  $d$  is the distance from the perpendicular center of the sphere, and  $\ell$  is the calculated path length.

Because there is only one factor of length in the equation for the Voigt Effect, the measured rotation for any calculated path length can be compared to the longest possible path length (the sphere's radius) with a proportion:

$$\phi_v = \frac{2r}{\ell}\phi_{v'}.$$

# Chapter 3

## Experimental Technique

### 3.1 Faraday Rotation

The experimental set-ups are shown in Figures 3.1 and 3.2. Two different instruments are used to measure polarization in this experiment: a balanced photodiode and a polarimeter. First, a photodiode system was used (Fig 3.1). An oven heats the alkali vapor, and the pump laser polarizes it. The probe laser points parallel to the  $B$ -field and is used to measure the Faraday Rotation (FR). It passes through a linear polarizer, then the cell, then through a beam-splitter cube that decomposes the linearly polarized light into vertical and horizontal components. The intensity of these two sources of light is measured using a balanced photodiode. The balanced photodiode produces a signal from each photodiode and a signal proportional to the difference between them. A chopper and lock-ins are implemented to prevent any other light from affecting the detected intensities. The asymmetry of the two intensity signals is related to the Faraday Rotation angle.

Next, the balanced photodiode was replaced with a Thorlabs polarimeter (Fig 3.2). Instead of passing through a beam-splitter cube, the polarization angle and power of the probe laser are measured directly using a polarimeter. The difference between the angle measured by the polarimeter and the angle of incident light is equal

**FR: Photodiode System**

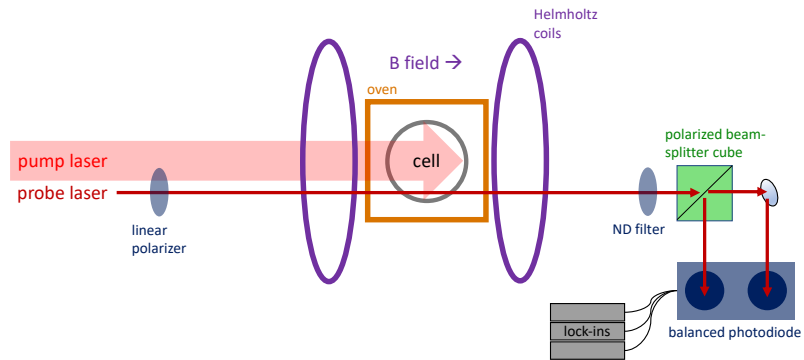


Figure 3.1: **Experimental Set-up: FR Photodiode System.** The pump and probe laser travel parallel to each other through the cell within the magnetic field created by the Helmholtz coils. The probe laser passes through a beam-splitter cube that decomposes it into horizontal and vertical components of linearly polarized light. The beam intensities are measured by a balanced photodiode.

to the Faraday Rotation angle.

## 3.2 Voigt Effect

This experimental set-up is shown in Figure 3.3. In this case, the probe laser is positioned normal to the  $B$ -field and is used to measure the Voigt Effect. To produce the largest signal, the initial linear polarization of the probe laser is set to 45 degrees. Downstream from the cell, the polarization angle and power are again measured with the polarimeter. The difference between the angle measured by the polarimeter and the angle of incident light is proportional to the rotation angle produced by the Voigt Effect (VR).

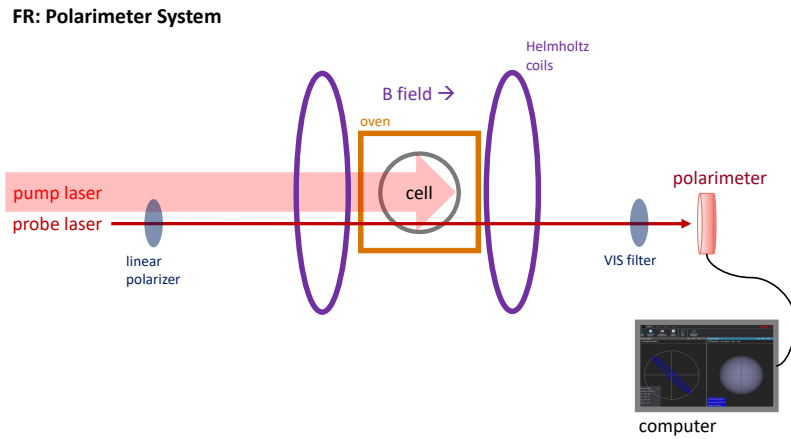


Figure 3.2: **Experimental Set-up: FR Polarimeter System.** The pump and probe laser travel parallel to each other through the cell within the magnetic field created by the Helmholtz coils. The probe laser angle and power are measured by a polarimeter.

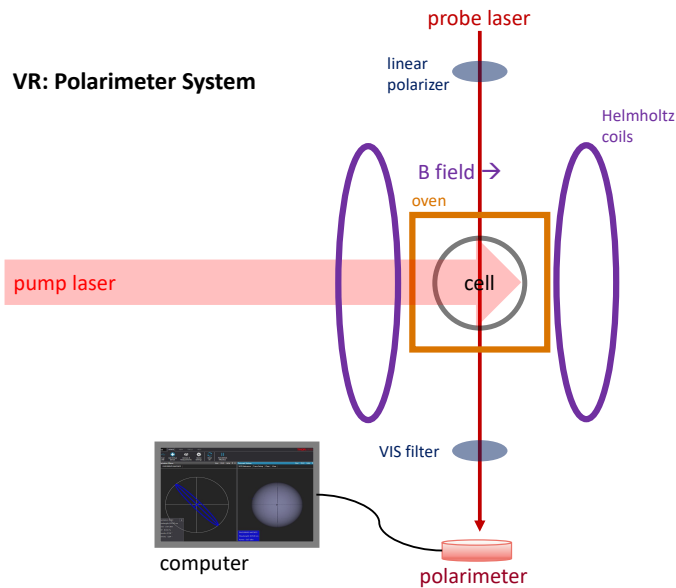


Figure 3.3: **Experimental Set-up: VR Polarimeter System.** The pump and probe laser travel normal to each other through the cell within the magnetic field created by the Helmholtz coils. The probe laser angle and power are measured by a polarimeter.

# Chapter 4

## Results and Conclusions

### 4.1 Results

#### 4.1.1 Simulated Faraday Rotation

Figures 4.1, 4.2, and 4.3 show the results of a preliminary test of the balanced photodiode system. The Faraday Rotation due to alkali vapor in the cell was simulated using a half-wave plate, which was rotated 360 degrees while measurements were taken from the balanced photodiode. Figure 4.1 depicts oscillations in intensities of the horizontal and vertical linearly polarized light, showing that the balanced photodiode captured the simulated rotation. Figure 4.2 depicts the asymmetry of the signal calculated in two different ways. In the first method, the difference is found by directly subtracting the two photodiode signals. In the second, the diff signal is used as the difference. The changing asymmetry confirms that it is related to Faraday Rotation and can be measured with the current system. Figure 4.3 depicts the linear relationship between the diff signal and the calculated difference of the photodiode signals, showing that the diff signal can be used in place of the calculated difference.

#### 4.1.2 Faraday Rotation

Figures 4.4 and 4.5 show the results of varying the pump laser power to change the alkali polarization. Figure 4.4 depicts changes in the intensities of the horizontal



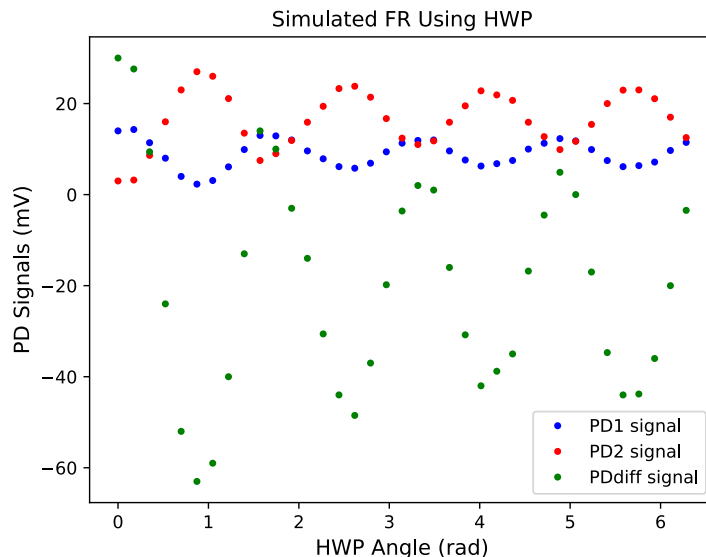


Figure 4.1: **Photodiode signals from simulated Faraday Rotation using a half-wave plate.** The two signals from the photodiodes represent the intensities of the linearly polarized light after being passed through a beam splitter cube that decomposed it into horizontal and vertical linear polarization. The changing intensities indicate changes in horizontal and vertical linear polarization, showing that they oscillated as the half-wave plate was rotated.

and vertical linearly polarized light. Figure 4.5 depicts how the asymmetry changes. These results indicate that the Faraday angle is indeed changing as the alkali polarization changes, and is measurable with this system, meaning that it is possible to find the spatial variability of the alkali polarization by measuring Faraday Rotation in different locations of the cell.

### 4.1.3 Voigt Effect

Figure 4.6 shows the results of varying the alkali polarization by changing the polarization of the pump laser from linear to circular. This test was done with different probe laser wavelengths. It indicates that, like Faraday Rotation, the Voigt Effect produces a larger rotation range for probe wavelengths closer to a resonance. The

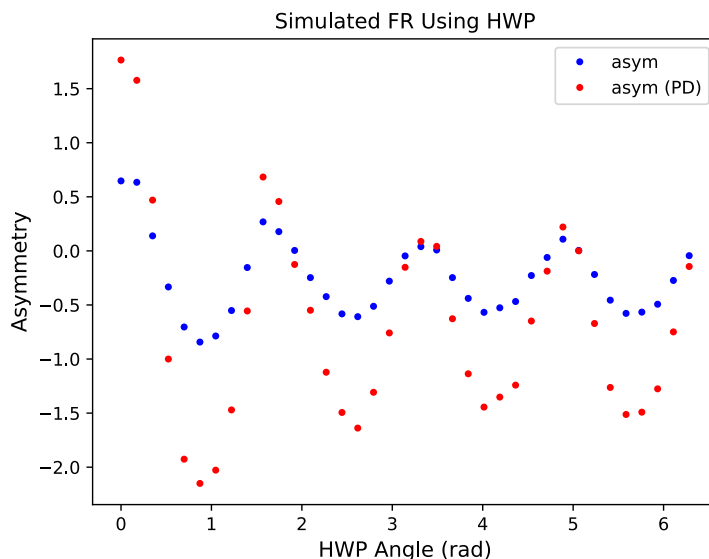


Figure 4.2: **Calculated asymmetry from simulated Faraday Rotation using a half-wave plate.** Calculated asymmetry from simulated Faraday Rotation using a half-wave plate. The asymmetry refers to the difference between the two signals divided by the sum. The difference was calculated by subtracting the two signals (asym) and by using the diff signal from the photodiode (PD asym).

ideal probe wavelength for measurement should show enough variation in rotation angle that differences in polarization can be easily detected, but without rotating too far because there is no way to distinguish between a 10-degree rotation and a 370-degree rotation. 793.77nm is determined to be the ideal wavelength for measurement. Wavelengths closer to resonance appear to rotate past 360 degrees.

Figure 4.7 shows the results of varying the alkali polarization by changing the pump laser power. These results, like Figure 4.5, indicate a direct relationship between the alkali polarization and the measured rotation due to the Voigt Effect, measurable by this system.

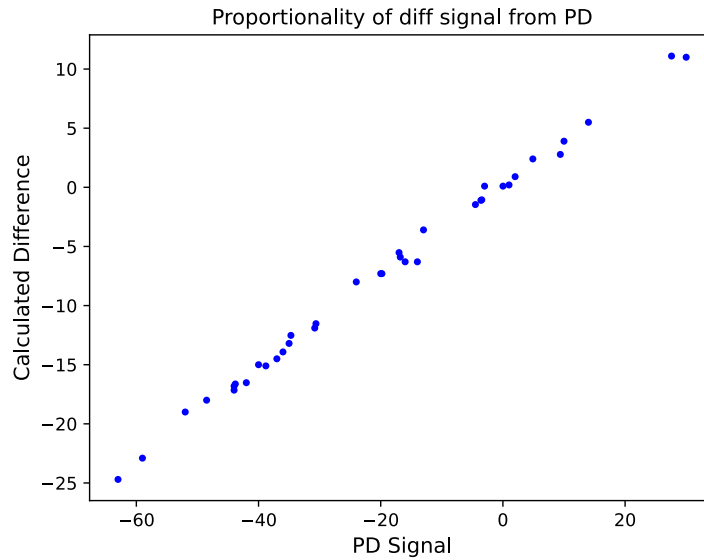


Figure 4.3: **Relationship between PD diff signal and difference.** The diff signal produced by the photodiode is proportional to the difference between the signals from each photodiode. The relationship is strongly linear, allowing the calculated difference to be replaced by the diff signal in future calculations.

Figure 4.8 shows the results of measuring VR from front to back across the center of the cell at different pump laser powers. The measured rotation due to the Voigt Effect changes when the probe laser is moved, even when controlling for different path lengths through the alkali vapor. These results indicate that the polarization in the cell may be non-uniform, with more polarization on the side facing the pump laser. This is similar to the distribution of D2 fluorescence in the cell from Figure 1.1.

The same test in Figure 4.8 was conducted again in Figure 4.9, but while the pump laser was aimed at both the front and back of the cell. This changed the distribution of D2 light (Figure 4.10) and the alkali polarization in a similar manner.

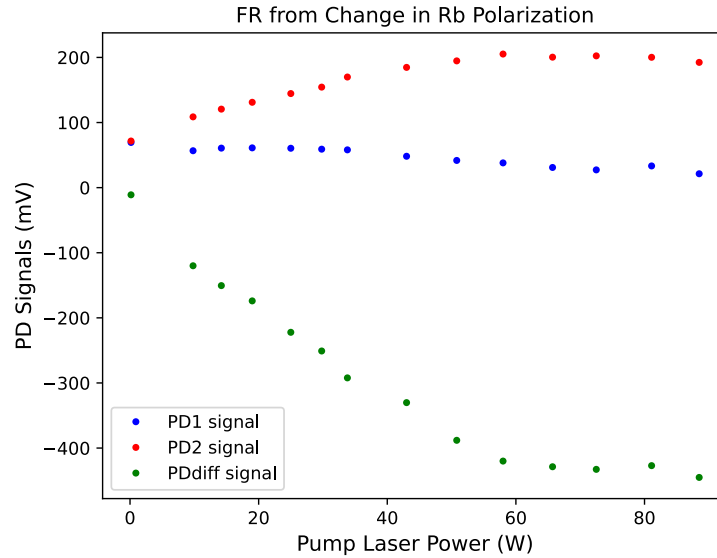


Figure 4.4: **Photodiode signals from Faraday Rotation due to change in alkali polarization.** The changing intensities indicate changes in horizontal and vertical linear polarization.

## 4.2 Error Analysis

There are many possible systemic errors in this experiment. The equations for Faraday Rotation and the Voigt Effect both depend on the alkali vapor density, which varies with temperature. Ideally, the cell would remain at a constant temperature but this is difficult to maintain because it is heated by both the oven and the pump laser. The oven can be set to a constant temperature, but the heat from the pump laser decreases as the power is decreased, resulting in an unaccounted for variable. However, data was taken quickly enough that the temperature only dropped slightly as the pump laser power was decreased.

The equation for path length correction assumes that the axis used for scanning the cell from front to back is in the exact center of the cell vertically. It also assumes that the probe laser passes through the cell exactly perpendicular to the scanning

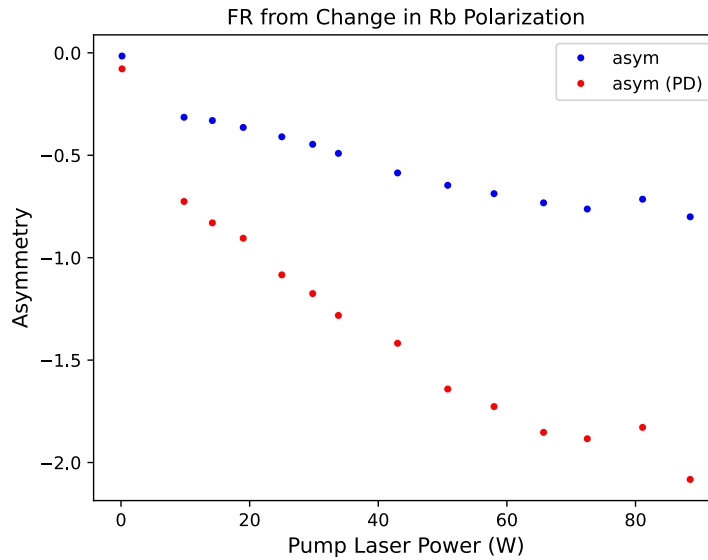


Figure 4.5: **Calculated asymmetry from Faraday Rotation due to change in alkali polarization.** The changing asymmetries show that the Faraday Rotation angle changes when the alkali polarization is increased.

axis, and that each positional measurement is taken in the exact same location. If any of these assumptions were incorrect, the true path length would be different than the calculated length used. However, small deviations in path length would cause equally small deviations in the results because the distance traveled by the probe laser through alkali vapor contributes linearly to the equations for Faraday Rotation and Voigt Effect.

Small imperfections in the spherical shape of the cell or in the glass could also affect the results.

### 4.3 Plans for Future Work

The next steps are to compare these results to the measured D2 fluorescence in the cell, and to a 3D simulation of alkali polarization in the cell. Further, multiple

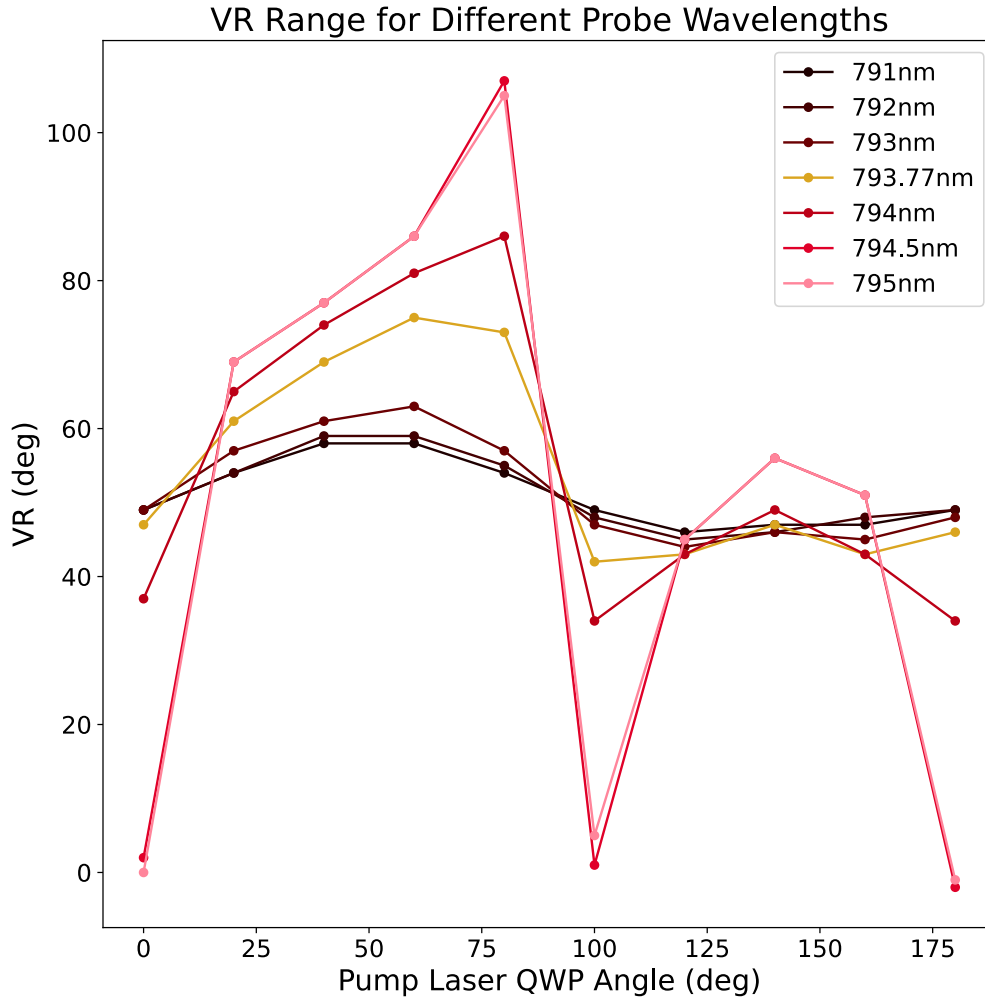


Figure 4.6: **VR range for different probe wavelengths.** Voigt Effect produces larger rotation range for wavelengths closer to resonance. Ideal probe wavelength for measurement is 793.77nm. Wavelengths closer to resonance appear to rotate past 360 degrees.

cells can be used to confirm the pattern of results.

To reduce possible errors, a cylindrical cell can be used to remove the need for a path length correction and allow for a more direct comparison between the D2

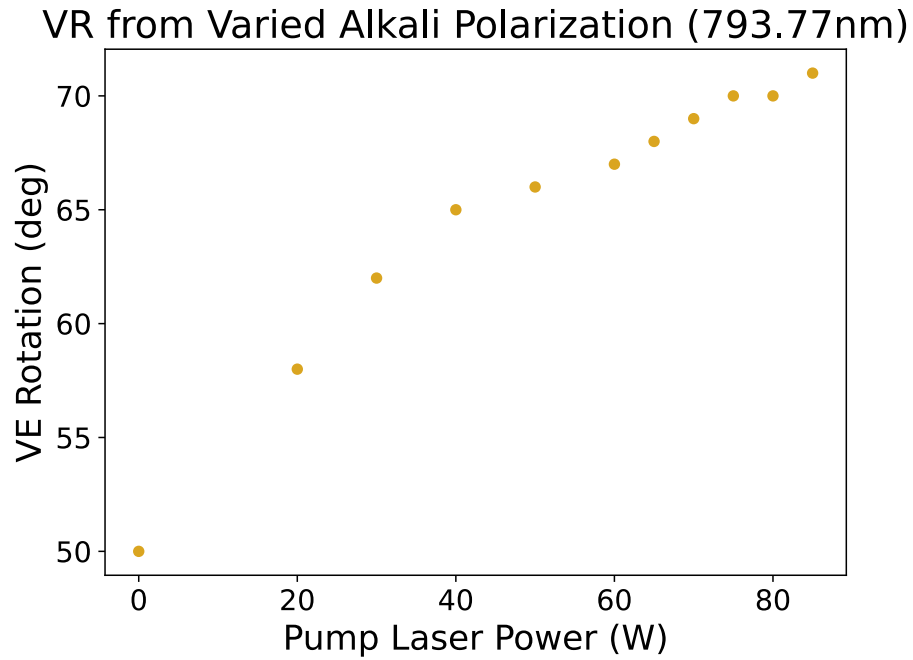


Figure 4.7: **VR from varied alkali polarization (793.77nm)**. The VR angle increases as alkali polarization (controlled by pump laser power) increases. Probe wavelength of 793.77nm is used.

fluorescence and the measured polarization. Multiple probe lasers could also be used to take data from multiple locations in the cell simultaneously.

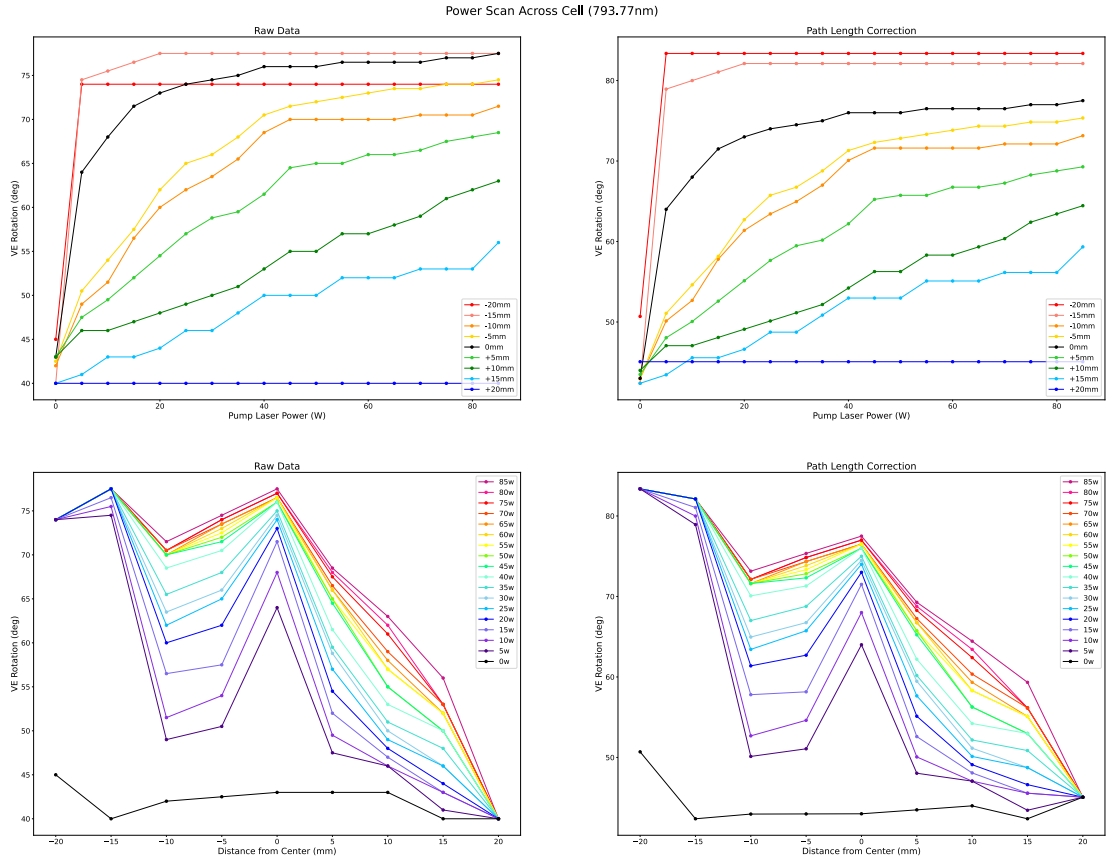


Figure 4.8: **VR across cell at varied pump laser power (793.77nm)**. Data is shown in two formats: grouped by location in cell above, and by pump laser power below. Raw data is shown on the left, and data corrected for path length is shown on the right. The VR angle varies at different locations, indicating that alkali polarization in the cell is non-uniform. Probe wavelength of 793.77nm is used.



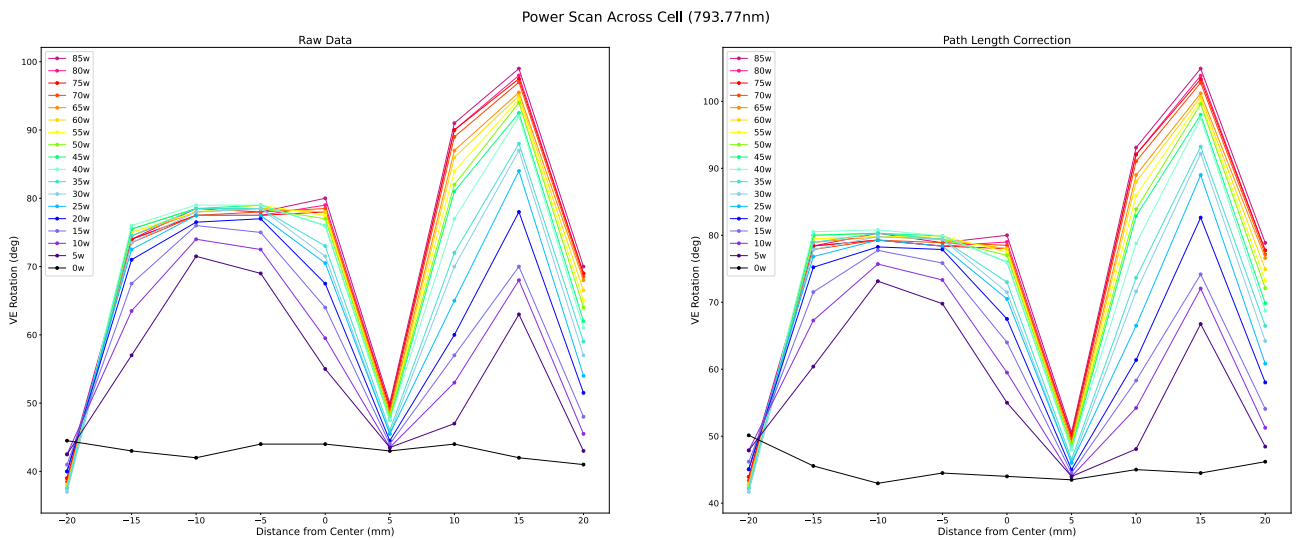


Figure 4.9: **VR across cell at varied pump laser power (pumped both sides, 793.77nm)**. The pump laser hits both the front and the back of the cell. The VR angle again varies at different locations, indicating that alkali polarization in the cell is non-uniform. Probe wavelength of 793.77nm is used.

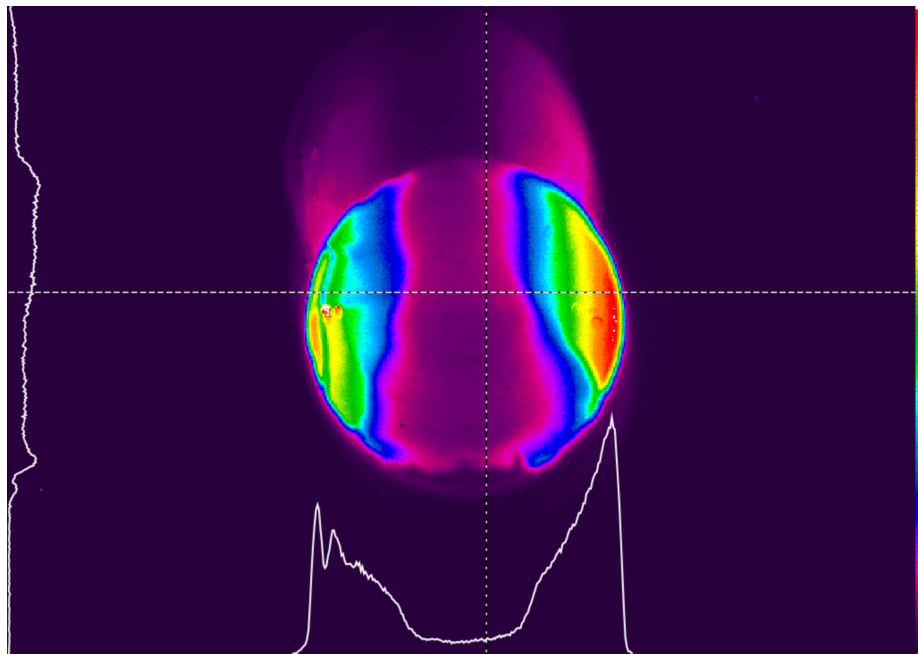


Figure 4.10: **D2 Fluorescence in a Cell (both sides)**. D2 fluorescence in a spherical cell measured during optical pumping from both sides of the cell. Light intensity is indicated with a color gradient. The light is concentrated on either side of the cell but not in the center.

# References

- [1] Gentile, T. R., Nacher, P. J., Saam, B., Walker, T. G. (2017). Optically polarized  $^3\text{He}$ . *Rev. Mod. Phys.*, 89, 045004. doi:10.1103/RevModPhys.89.045004.
- [2] Chann, B., Babcock, E., Anderson, L. W., Walker, T. G. (2002). Measurements of  $^3\text{He}$  spin-exchange rates. *Phys. Rev. A*, 66, 032703. doi:10.1103/PhysRevA.66.032703.
- [3] Ben-Amar Baranga, A., Appelt, S., Erickson, C. J., Young, A. R., Happer, W. (2002). Alkali-metal-atom polarization imaging in high-pressure optical-pumping cells. *Phys. Rev. A*, 58, 2282.
- [4] Michael A. Cario. Studies in SEOP hyperpolarized  $^3\text{He}$ : measuring  $k_0$  and the spatial dependence of alkali polarization. William and Mary Bachelor's Thesis, May 2020.
- [5] Peter M. Dolph. High-performance nuclear-polarized  $^3\text{He}$  targets for electron scattering based on spin-exchange optical pumping. University of Virginia Doctoral Thesis, December 2010.
- [6] Franke-Arnold, S., Arndt, M., Zeilinger, A. (2001). Magneto-optical effects with cold lithium atoms. *Phys. B: At. Mol. Opt. Phys*, 34, 2527.